journal

J. Am. Ceram. Soc., 86 [7] 1094–98 (2003)

Fabrication and Evaluation of Porous Piezoelectric Ceramics and Porosity-Graded Piezoelectric Actuators

Jing-Feng Li,*,†,‡ Kenta Takagi,‡ Masaru Ono,‡ Wei Pan,† and Ryuzo Watanabe‡

State Key Laboratory of New Ceramics and Fine Processing, Department of Materials Science and Engineering, Tsinghua University, Beijing 100084, People's Republic of China

Department of Materials Processing, School of Engineering, Tohoku University, Sendai, Japan

Abdulhakim Almajid and Minoru Taya

Center for Intelligent Materials and Systems, Department of Mechanical Engineering, University of Washington, Seattle, Washington

Porous ceramics of lead zirconate titanate (PZT) were prepared by sintering powder compacts consisting of PZT and stearic acid powders in an air atmosphere; stearic acid was added as a pore-forming agent (PFA). The dielectric, elastic and piezoelectric properties of uniformly porous PZT ceramics were investigated as a function of the porosity volume fraction. Furthermore, a beam-shaped PZT actuator sample with a graded porosity content across its thickness was fabricated by sintering PFA-graded powder compacts. The electric-field-induced bending displacement characteristics of the actuator samples were measured by using strain gauges and were found to be in good agreement with the theoretical predication based on a classical lamination theory.

I. Introduction

PIEZOELECTRIC actuators are technologically important in the fields of smart materials and microelectromechanical systems (MEMS). Unimorph and monomorph actuators are two well-known types of piezoelectric actuators, which use a flexural mode to produce larger displacements compared with extensional-mode actuators.[1] Conventional unimorph and monomorph actuators consist of piezoelectric plates and metal shims that are bonded together with an organic agent (usually epoxy resin). The inherent problem associated with such actuators is deterioration of the bonding strength after a long period of use.[1] The concept of functionally graded materials (FGM) is expected to be a good solution to this problem.[2–10] Numerical and theoretical analyses[4,5] show that FGM piezoelectric actuators exhibit lower mechanical stresses while producing electrically induced displacements comparable to that of conventional bimorph actuators. Some studies have been devoted to the fabrication of FGM piezoelectric actuators. For example, Zhu and Meng[6] have developed an FGM actuator with a compositional gradient from high piezoelectric–low dielectric material to low piezoelectric–high dielectric material. Wu *et al.*[7] fabricated a piezoelectric monomorph actuator that has graded electrical resistances through the plate thickness due to the controlled diffusion of zinc borate (ZnB).

The present work focuses on the development of a new type of FGM piezoelectric actuator that has a porosity gradient across the thickness. The porosity gradient is formed *in situ* by sintering layer-stacked PZT powder compacts with stepwise varied contents of stearic acid as a pyrolyzable pore-forming agent (PFA),[11] which is burned out during sintering. The resultant ceramic plates with the graded porosity are expected to behave like a monolithic piezoelectric bender producing bending displacements when an electric field is applied in the thickness direction, because the piezoelectric and elastic properties were gradually reduced through the plate thickness with increasing porosity. In the present study, monolithic piezoelectric ceramics with various porosities are prepared and their piezoelectric properties are investigated as a function of porosity, and the electric-field-induced bending displacement characteristics of the porosity-graded samples are evaluated and analyzed based on a modified classical lamination theory.

II. Experimental Procedure

Commercially available PZT (LQ-PZT, Zr/Ti atomic ratio = 0.516/0.484; average particle size: 0.97 μm; Sakai Chemicals Co. Ltd., Japan) powder and stearic acid ($CH_3(CH_2)_{16}COOH$, Wako Pure Chemical Industries, Ltd., Japan) powder[§] were used as the starting materials. Predetermined amounts of stearic acid were added to PZT powders and mixed in an alumina mortar with a pestle. The mixed powders were compacted by die pressing at 100 MPa, and subsequently by cold isostatic pressing at 200 MPa. The green compacts with different amounts of stearic acid powder were sintered in air at 1473 K for 1 h, in a covered Al_2O_3 (99.9% purity) crucible that contained $PbZrO_3$ powder to produce an excess-PbO atmosphere. The heating rates were 5 K/min from room temperature to 473 K, 1 K/min from 474 to 573 K, and 10 K/min from 573 to 1473 K to ensure the complete and "mild" pyrolysis of stearic acid. The sintering shrinkage rate was measured as a function of temperature using a dilatometer. Bulk density (ρ) was determined by the Archimedes method, and converted to a relative value of the theoretical density (ρ_t = 8.0 g/cm^3 based on XRD Card No. 33-0784) for the PZT ceramics, and bulk porosity (including open and closed porosity), P_b, was calculated using the formula P_b =

W. A. Schulze—contributing editor

Manuscript No. 187412. Received October 10, 2001; approved January 28, 2003.
Presented partly at the 6th International Symposium on Functionally Graded Materials, Estes Park, CO, September 10–14, 2000.
This research has received financial support from the National Natural Science Foundation (Grant No. 50242016) and the Ministry of Science and Technology of China (Grant No. 20002CB613306) to Tsinghua University and also from a NEDO contract on Smart Materials and Structures to the University of Washington.
*Member, American Ceramic Society.
†Tsinghua University.
‡Tohoku University.

§The as-received stearic acid powder looked quite coarse because it was softly granulated. After being mixed with the PZT powders, the average diameter of the stearic acid powder was measured to be 18.36 μm by using a laser particle size analyzer.

$1 - \rho/\rho_t$. The open porosity (P_o) was determined by measuring weight difference of the specimen before and after being saturated with boiling water, and the closed porosity (P_c) was then calculated from the relation $P_c = P_b - P_o$. The microstructure was observed using scanning electron microscopy (SEM).

The specimens used for measuring piezoelectric properties were machined according to EMAS-6100, the standard of the Electronic Materials Manufacturers Association of Japan.[12] After silver paste electrodes were formed on appropriate surfaces, the specimens were poled under a dc field of 1–2 MV/m at 393 K for 60 min in a bath of silicone oil. The poled specimens were ultrasonically rinsed using an acetone solution to remove the immersion oil. The piezoelectric properties of the poled specimens were measured using an impedance/gain phase analyzer (Model HP4194A, Hewlett-Packard). The polarization (P) vs electric field (E) curves were measured for the nonpolarized specimens using a Radiant RT6000HVS ferroelectric test system.

The FGM samples were prepared by the following powder metallurgical process: stacking the powder mixtures with various compositions in a carbon steel die 16 mm in diameter, and then compacting under a pressure of 200 MPa and sintering in air at 1473 K for 1 h. Beam-shaped actuators with dimensions of 12 mm × 3 mm × 1 mm were cut from the sintered disk, and two large rectangular surfaces were polished using No. 800 SiC paper. Such samples with silver paste (mixed with frit) electrodes on the polished surfaces were poled in the same way for the uniform porous samples as mentioned above. Two lead wires were connected to the silver paste electrodes, and two strain gauges (2 mm long × 1 mm wide) were mounted on the centers of the two surfaces. The strains of the two surfaces were recorded and converted to the curvature and hence the bending displacement of the actuator, when it was subjected to a dc electric voltage.

III. Results and Discussion

(1) Porous PZT Ceramics

Figure 1 shows the shrinkage curves of the powder compacts containing various volume fractions of stearic acid as a function of temperature. The powder compacts containing 0–40 vol% stearic acid showed similar shrinkage curves; the starting temperatures of densification and total shrinkage were almost the same. Because sintering densification occurred in the ceramic powder matrix (surrounding the PFA particulates) whose packing density was probably unchanged by the addition of PFA, the resultant shrinkage remained almost the same in all of the green compacts. However, when the stearic acid addition was more than 50 vol%, the excess amount of stearic acid, which has a low melting point (341–344 K) and boiling point (633 K), significantly reduced the rigidity of the powder compacts. Consequently the powder compact containing 60 vol% stearic acid was distorted because of the small pressure from the detecting bar of the dilatometer, resulting in an apparent large shrinkage at temperatures as low as 500 K. Therefore, the volume fraction of stearic acid was limited to less than 50% in the following experiments.

By density measurements, it was found that the powder compact without stearic acid was sintered to 97.48% of the theoretical density at 1473 K for 1 h. Under the same conditions, 22.52% porosity was produced in the sample containing 40 vol% stearic acid. Figure 2 shows the change in bulk and open porosities as a function of the volume fraction of stearic acid, for the samples sintered at 1473 K for 1 h. The bulk porosity increased almost linearly with increasing PFA volume fraction, but it was smaller than the expected porosity (shown by the straight line in the figure) based on the volume fraction of stearic acid in the powder compacts. These results seem to contradict those obtained by Corbin and Apte,[11] who found that porosity generated in their tape-cast ZrO_2 preforms was larger than the volume fraction of PFA in the green body. Different results were obtained in the present study because of the following fact. As known from its use in lubricants for powder die pressing, stearic acid particles are fairly soft and deformable; consequently some compress and coat the PZT powders during the mixing and compacting processes. A portion of such small voids generated by the stearic acid pyrolysis disappear during the sintering process at sufficiently high temperatures. That is the reason that the obtained porosity was lower than the volume fraction of stearic acid added in the powder compact. On the other hand, Corbin and Apte reported that[11] the particle sizes of PFAs were much larger than those of the matrix ZrO_2 powder; as a result the sintering process was unable to eliminate such large voids.

Figure 3 shows the SEM micrographs of the polished surfaces of the sintered PZT samples with and without PFA additions. From this figure, one can easily envisage that the large pores were the spaces occupied by the stearic acid particles. Most of the PFA-derived pores had elongated cross-sections with a long axis of 10–30 μm, suggesting that the stearic acid particles were deformed during the die-pressing process. The small pores observed in the sample without PFA are the residual sintered pores of the PZT ceramics.

The dielectric, elastic, and piezoelectric properties were measured as a function of porosity using the samples sintered at 1473 K for 1 h. Figure 4 shows the P–E hysteresis loops of the PZT

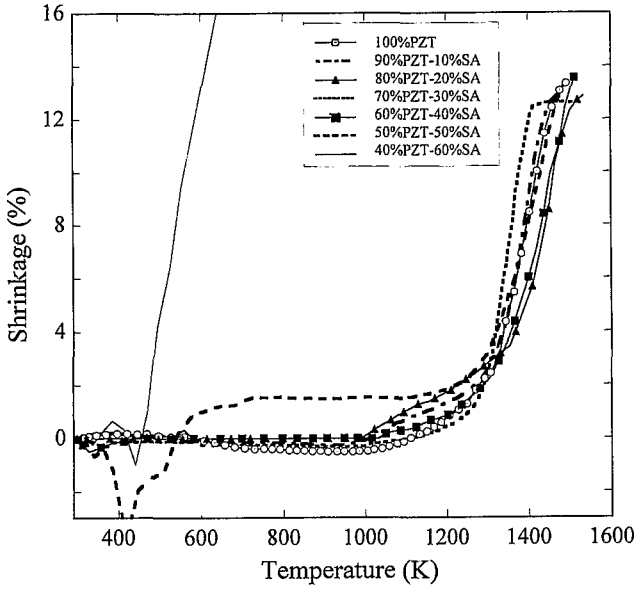

Fig. 1. Shrinkage curves of powder compacts of PZT and stearic acid (SA) with different ratios as a function of temperature.

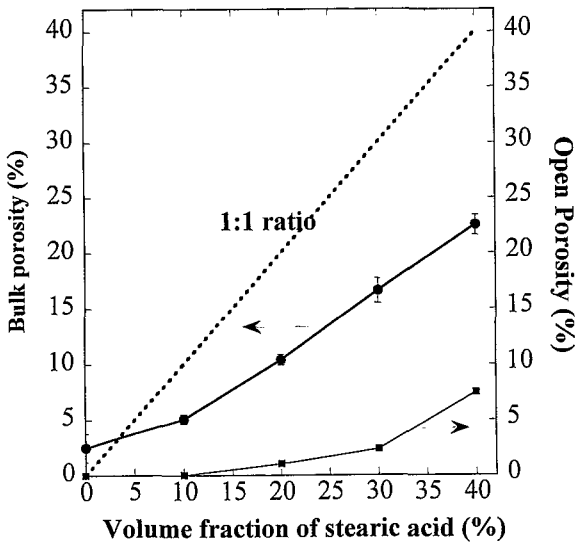

Fig. 2. Change in bulk and open porosities as a function of the volume fraction of stearic acid in the green compacts.

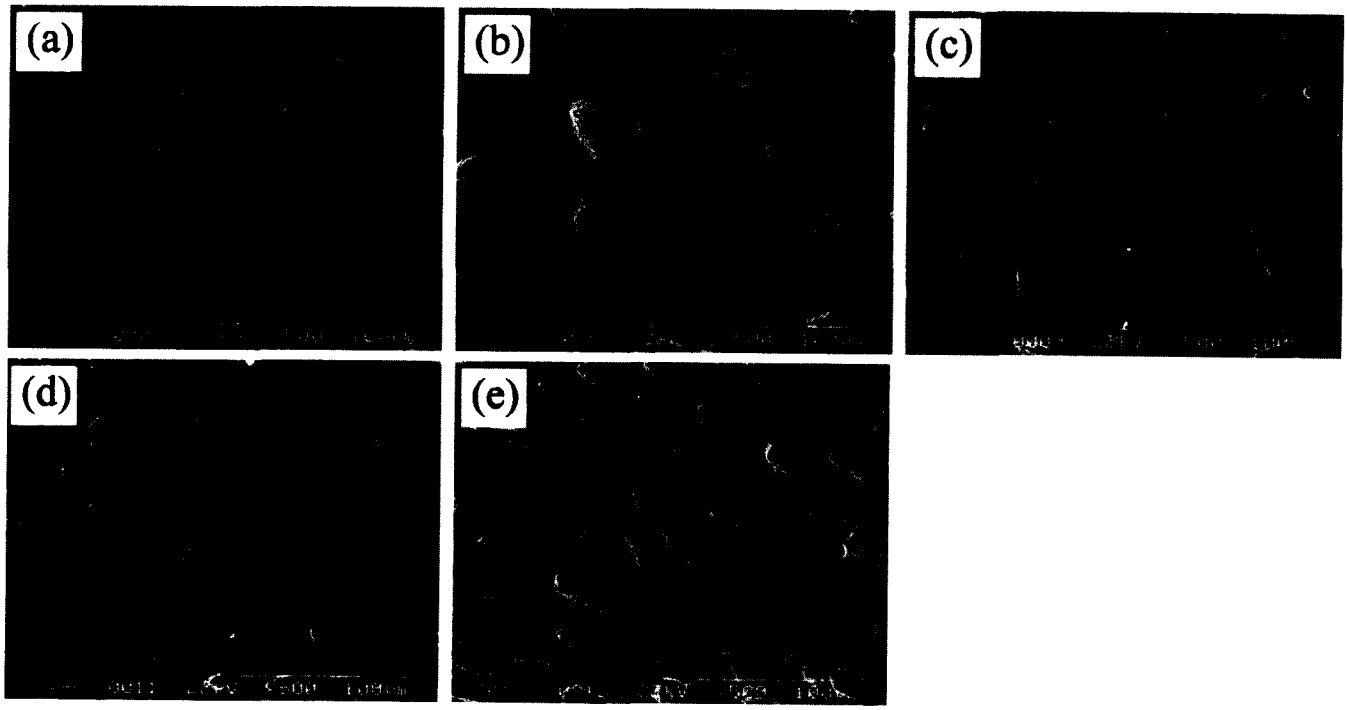

Fig. 3. SEM micrographs of the cross sections of PZT ceramics sintered at 1473 K for 1 h. The volume fractions of stearic acid in the green compacts are (a) 0%, (b) 10%, (c) 20%, (d) 30%, and (e) 40%.

ceramics with 30% PFA and without PFA. The residual polarization (P_r) decreased from 43 to 18 μC/cm^2 as the porosity was increased from 2.52% to 16.62%, whereas the coercive field (E_c) remained unchanged regardless of porosity. This result suggests that the base PZT phases in both samples have almost the same ferroelectric properties, regardless of the existence of the intentionally added porosity. The change of relative dielectric constants as a function of porosity is shown in Fig. 5, in which the theoretically predicted data are shown by the lines. Note that the measuring direction was parallel to the die-pressing direction for the powder compaction, i.e., perpendicular to the long axis direction of the pores as shown in Fig. 3. The relative dielectric constants ($\varepsilon_{33}^T/\varepsilon_0$) of the porous PZT samples were computed from the value ($\varepsilon_{33}^T/\varepsilon_{0(p=0)}$) for the PZT ceramics without PFA according to the following equation:[13]

$$\varepsilon_{33}^T/\varepsilon_0 = (\varepsilon_{33}^T/\varepsilon_{0(p=0)})\left\{1 + \left[\frac{1}{p^{1/3}(\varepsilon_{33}^T/\varepsilon_{0(p=0)} - 1)K_s^{2/3} + 1}\right]\frac{p^{2/3}}{K_s^{2/3}} - \frac{p^{2/3}}{K_s^{2/3}}\right\} \quad (1)$$

where p is porosity and K_s a parameter that is dependent on the shape of a pore. For a spherical pore, $K_s = 1$; for an oval pore, $K_s = \sim 0.5$.

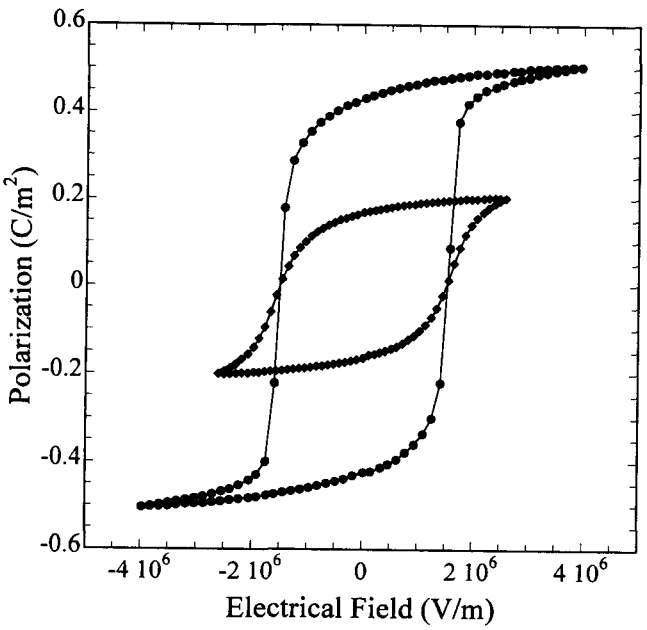

Fig. 4. Polarization–field hysteresis loops of 97.47% dense PZT (circles) and 83.38% dense PZT (diamonds) ceramics.

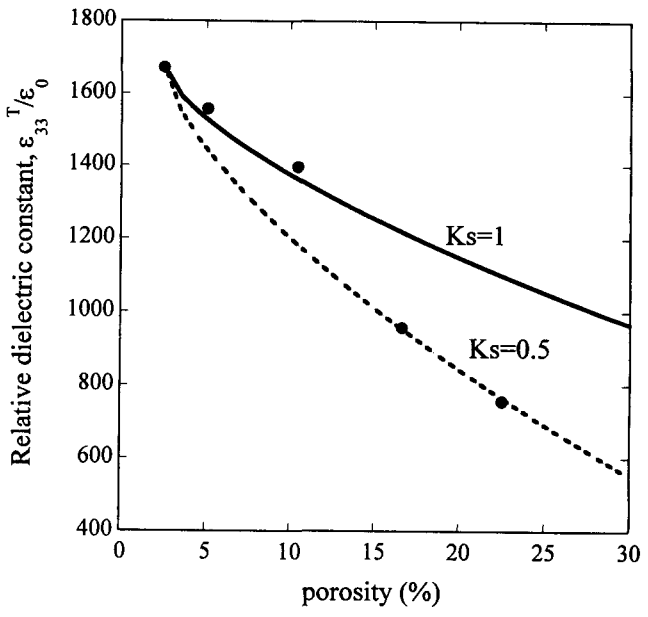

Fig. 5. Relative dielectric constants of PZT ceramics as a function of bulk porosity. The lines are the predicted values from Eq. (1) for two typical shapes of pores.

Table I. Piezoelectric and Elastic Constants of PZT Ceramics with Different Amounts of Bulk Porosity

Porosity (%)	d_{31} (pC/N)	d_{33} (pC/N)	k_{31}	c_{11} (GPa)	c_{12} (GPa)	c_{66} (GPa)	e_{31} (C/m^2)
0.23	−181	451	0.38	142	94.6	23.8	−5.17
4.25	−150	420	0.31	110	65.8	22	−3.49
9.47	−122	436	0.25	86.1	46.8	19.6	−0.97
14.41	−75.9	377	0.18	74.1	38.2	18	0.46
20.82	−47.2	350	0.12	58.7	27.2	15.8	1.93

As shown in Fig. 5, the measured data are located between the two predicted bounds for $K_s = 0.5$ and 1.0, and a better agreement was obtained between the measured data and predicted values for the samples with >10% porosity. It is unclear why good agreements were obtained separately in two different ranges, but one possible reason may be related to the fact that open porosity increased when the porosity exceeded 10%, as shown in Fig. 2.

Table I summarizes the piezoelectric and elastic constants of the nearly dense and porous PZT ceramics after poling. As expected, the elastic and piezoelectric constants were monotonically reduced with increasing porosity. Tuttle *et al.*[14] have particularly investigated the effect of porosity on the elastic constants of PZT ceramics using the acoustic method. In this study, the elastic constants were computed from the resonant and antiresonant frequencies of the impedance curves. As compared with the porosity dependence of elastic constants obtained by Tuttle *et al.*,[14] the elastic constants decreased more for the same porosity of the samples. The reason for this difference is not clear. A PZT plate with graded porosity through the thickness can be used as a monolithic actuator like a RAINBOW actuator,[15] which is produced by reducing one surface of a PZT wafer.

(2) FGM Actuators

Disk-shaped FGM piezoelectric bending actuators with five layers, in which the volume fractions of stearic acid were varied from 0 to 40 vol% at intervals of 10 vol%, were formed and sintered at 1473 K for 1 h, resulting in the *in situ* formation of a monolithic porosity-graded PZT disk. As revealed in the PZT/Pt system,[16] the maximum piezoelectric effect can be realized in an FGM actuator with a linear gradient profile. The resultant samples were crack-free with flat surfaces because each layer shrank during sintering at nearly the same rate as shown in Fig. 1. Figure 6 shows the cross section of the FGM sample of five layers, in which each layer is 0.2 mm thick. By image analysis of SEM micrographs, the porosity in each layer was measured to be 2.4%, 5.0%, 11.4%, 16.9%, and 21.4% from the dense to porous side, being almost equal to that obtained in the nongraded porous samples for the same volume fraction of stearic acid.

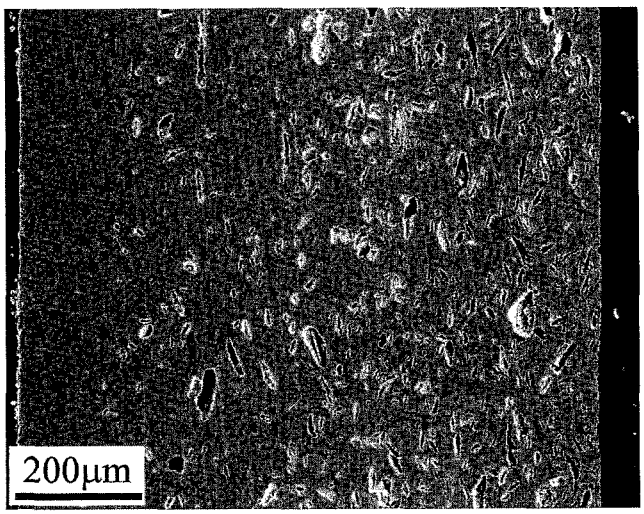

Fig. 6. SEM micrograph of the fabricated PZT sample with a linear porosity gradient.

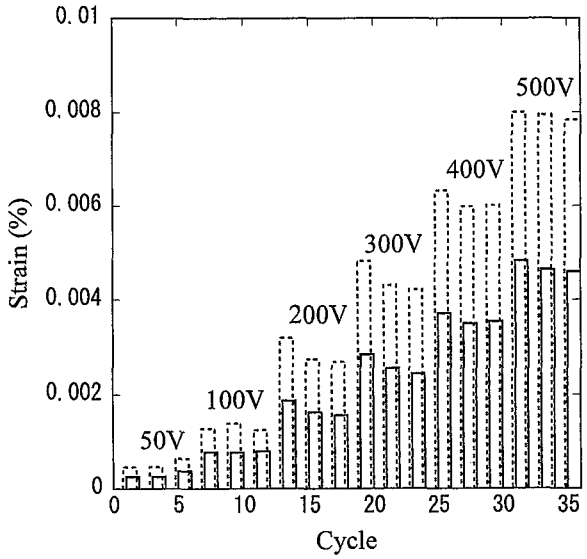

Fig. 7. Measured strains on the two sides (dotted lines: dense side; solid lines: porous side) of the FGM sample for different applied voltages from 50 to 500 V. Each voltage was repeated three times.

The electric-field-induced bending displacements of the above FGM actuators were measured using the strain gauges pasted on the two sides of the samples. Figure 7 shows the strains recorded by the two strain gauges, when the electric field was increased from 50 to 500 V in steps of 50 V. For each voltage, three cycles were applied. The strain data were converted to curvature (k) of the actuator by the following equation, and the results are shown in Fig. 8:

$$k = \frac{1}{t}\left(1 - \frac{1+\varepsilon_1}{1+\varepsilon_2}\right) \tag{2}$$

where ε_1 and ε_2 are the top and bottom strains, respectively, and t is the total thickness of the FGM sample.

As shown in Fig. 8, the curvature increases almost linearly with increasing voltage, reaching 0.032 m^{-1} at a maximum voltage of

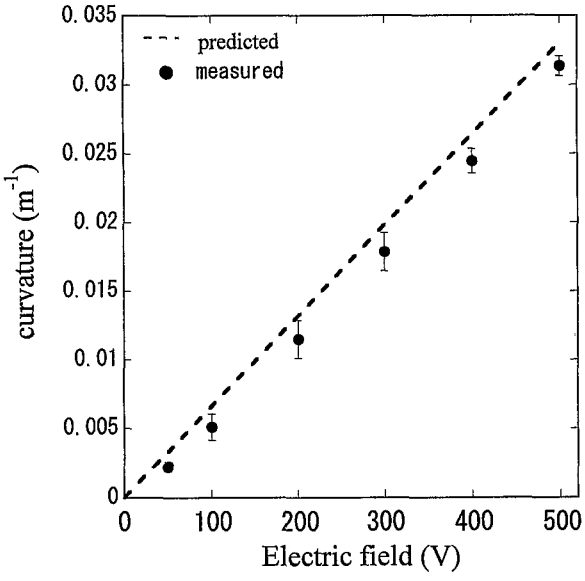

Fig. 8. Electric-field-induced curvature of the porosity-graded PZT beam-shaped actuator as a function of applied voltage.

500 V. The experimental data are in good agreement with the theoretically predicted values by a modified classical lamination theory[5] using the measured elastic and piezoelectric constants of the porous PZT ceramics with different porosities. For reference, the calculation procedure of the electric-field-induced curvature of a multilayered piezoelectric actuator is given in the Appendix, and the details can be found elsewhere.[5]

The corresponding end-point displacement at 500 V is calculated to be 2.3 μm, according to the following equation, if one end of the beam specimen is fixed:

$$\delta = \frac{1}{2}(kl^2) \tag{3}$$

where δ is displacement, and l is specimen length. By comparing the results of Fig. 8 with similar results reported in the literature,[6] it was found that the present porous FGM actuators can produce equivalent displacement as the dielectric–piezoelectric FGM actuators developed by Zhu and Meng,[6] provided that the specimen dimensions and the applied voltage are identical. However, the gradient profiles of their FGM actuators are difficult to control because the compositional distribution is greatly affected by the interdiffusion between dielectric and piezoelectric ceramics. The porosity profiles in the present actuators can be varied over a wide range by adjusting the PFA distributions and sintering temperatures. More studies are in progress to further increase open porosity by testing other organics as PFAs or combining stearic acid powders with other PFAs, because open porosity-graded PZT plates can be used as preforms, into which metal and polymer phases are infiltrated to produce metal/PZT and polymer/PZT FGM actuators.

IV. Conclusions

Porous PZT ceramics have been fabricated by incorporating stearic acid powder as a pyrolyzable pore-forming agent (PFA) into PZT powder and normal sintering in air. Since porosity significantly reduces the dielectric, elastic, and piezoelectric constants of the PZT ceramics, a porosity-graded monolithic actuator similar to RAINBOW-type can be *in situ* fabricated by sintering a piezoelectric powder compact with a gradient of a pyrolyzable PFA across the thickness. In the present study, beam-shaped porosity-graded FGM actuators that were crack-free were successfully fabricated by normal sintering of the layer-stacked powder compacts with a PFA gradient. The processed FGM actuator samples exhibited electric-mechanical responses that were in good agreement with the theoretical predications.

Appendix

For a laminated FGM actuator under an applied field (E) across its thickness, the electric-field-induced curvature (k) can be computed from the following equation and matrixes using the piezoelectric constants and the thickness of each layer:[5]

$$\{k\} = [[A]^{-1}[B] - [B][D]^{-1}]\cdot[[A]^{-1}[N]^E - [B]^{-1}[M]^E]\cdot\{E\}$$

$$[A] = \sum_{i=1}^{n} \begin{bmatrix} \bar{Q}_{11} & \bar{Q}_{12} & 0 \\ \bar{Q}_{12} & \bar{Q}_{11} & 0 \\ 0 & 0 & \bar{Q}_{66} \end{bmatrix}_i (h_i - h_{i-1})$$

$$[B] = \frac{1}{2}\sum_{i=1}^{n} \begin{bmatrix} \bar{Q}_{11} & \bar{Q}_{12} & 0 \\ \bar{Q}_{12} & \bar{Q}_{11} & 0 \\ 0 & 0 & \bar{Q}_{66} \end{bmatrix}_i (h_i^2 - h_{i-1}^2)$$

$$[D] = \frac{1}{3}\sum_{i=1}^{n} \begin{bmatrix} \bar{Q}_{11} & \bar{Q}_{12} & 0 \\ \bar{Q}_{12} & \bar{Q}_{11} & 0 \\ 0 & 0 & \bar{Q}_{66} \end{bmatrix}_i (h_i^3 - h_{i-1}^3)$$

$$[M]^E = \frac{1}{2}\sum_{i=1}^{n} \begin{bmatrix} 0 & 0 & \bar{e}_{31} \\ 0 & 0 & \bar{e}_{31} \\ 0 & 0 & 0 \end{bmatrix}_i (h_i^2 - h_{i-1}^2)$$

$$[N]^E = \sum_{i=1}^{n} \begin{bmatrix} 0 & 0 & \bar{e}_{31} \\ 0 & 0 & \bar{e}_{31} \\ 0 & 0 & 0 \end{bmatrix}_i (h_i - h_{i-1})$$

where $h_i - h_{i-1}$ represents the thickness of the ith layer. $\bar{Q}_{ij}$ and $\bar{e}_{ij}$ are the reduced stiffness constants and reduced piezoelectric constants, respectively, that are associated with common stiffness constants (C_{ij}) and piezoelectric constants (e_{ij}) as follows:

$$\overline{Q_{ij}} = C_{ij} - \left(\frac{C_{i3}}{C_{33}}\right)C_{j3}$$

$$\overline{e_{ij}} = \left(\frac{C_{i3}}{C_{33}}\right)e_{33} - e_{ij}$$

Acknowledgments

We thank Sakai Chemicals Co. Ltd. Japan for providing the PZT powder.

References

[1]K. Uchino, "Materials Issues in Design and Performance of Piezoelectric Actuators: An Overview," *Acta Mater.*, **46** [11] 3745–53 (1998).

[2]M. Niino, T. Hirai, and R. Watanabe, "Functionally Gradient Materials—High Temperature Use for Space Rocket" (in Jpn.), *J. Jpn. Soc. Compos. Mater.*, **13**, 257–64 (1987).

[3]A. Kawasaki and R. Watanabe, "Finite Element Analysis of Thermal Stress of Metal/Ceramic Multilayer Composites with Controlled Compositional Gradients" (in Jpn.), *J. Jpn. Inst. Met.*, 51, 525–29 (1987).

[4]A. Kouvatov, R. Steinhausen, W. Seifert, T. Hauke, H. T. Langhammer, H. Beige, and H. Abicht, "Comparison Between Bimorphic and Polymorphic Bending Devices," *J. Eur. Ceram. Soc.*, **19**, 1153–56 (1999).

[5]A. Almajid, M. Taya, and S. Hudnut, "Analysis of Out-of-Plane Displacement and Stress Field in a Piezocomposite Plate with Functionally Graded Microstructure," *Int. J. Solids Struct.*, **38**, 3377–91 (2001).

[6]X. Zhu and Z. Meng, "Operational Principle, Fabrication and Displacement Characteristics of a Functionally Gradient Piezoelectric Ceramic Actuator," *Sens. Actuators A*, **48**, 169–76 (1995).

[7]C. C. Wu, M. Kahn, and W. Moy, "Piezoelectric Ceramics with Functional Gradients: A New Application in Material Design," *J. Am. Ceram. Soc.*, **79** [3] 809–12 (1996).

[8]T. Kawai, S.-I. Miyazaki, and M. Araragi, "A New Method for Forming a Piezoelectric FGM Using a Dual Dispenser System"; pp. 191–96 in Proceedings of the First International Symposium on Functionally Gradient Materials. Edited by M. Yamanouchi, M. Koizumi, T. Hirai, and I. Shiota. Functionally Gradient Materials Forum, Sendai, Japan, 1990.

[9]W. F. Shelley I. I., S. Wan, and K. J. Bowman, "Functionally Graded Piezoelectric Ceramics," *Mater. Sci. Forum*, **308–311**, 515–20 (1999).

[10]N. Terakubo, J.-F. Li, M. Ono, and R. Watanabe, "Fabrication of Functionally Graded PZT/Pt Piezoelectric Actuators" (in Jpn.), *J. Jpn. Soc. Powder Powder Metall.*, **47**, 1216–20 (2000).

[11]S. F. Corbin and P. S. Apté, "Engineered Porosity via Tape Casting, Lamination and the Percolation of Pyrolyzable Particulates," *J. Am. Ceram. Soc.*, **82** [7] 1693–701 (1999).

[12]Standard of Electronic Materials Manufacturers Association of Japan, EMAS-6100, 1993.

[13]H. Banno, "Effects of Shape and Volume Fraction of Closed Pores on Dielectric, Elastic, and Electromechanical Properties of Dielectric and Piezoelectric Ceramics—A Theoretical Approach," *Am. Ceram. Soc. Bull.*, **66** [9] 1332–37 (1987).

[14]B. A. Tuttle, P. Yang, J. H. Gieske, J. A. Voigt, T. W. Scofield, D. H. Zeuch, and W. R. Olson, "Pressure-Induced Phase Transformation of Controlled-Porosity $Pb(Zr_{0.95}Ti_{0.05})O_3$ Ceramics," *J. Am. Ceram. Soc.*, **84** [6] 1260–64 (2001).

[15]G. H. Haertling, "Rainbow Ceramics—A New Type of Ultra-High-Displacement Actuator," *Am. Ceram. Soc. Bull.*, **73** [1] 93–96 (1994).

[16]K. Takagi, J.-F. Li, S. Yokoyama, R. Watanabe, A. Almajid, and M. Taya, "Design and Fabrication of Functionally Graded PZT/Pt Piezoelectric Bimorph Actuator," *Sci. Technol. Adv. Mater.*, **3**, 217–24 (2002). □